

# The tropical circulation in the Australian/Asian region - May to October 2000

Hakeem A. Shaik and Peter W. Bate

Regional Office, Bureau of Meteorology, Darwin, Australia

(Manuscript received May 2001)

**A summary of the broadscale tropical circulation from 70°E to 180°, for the six months May to October 2000, is presented. Weak La Niña conditions persisted throughout the season. Evidence for this includes continuation of an enhanced upward branch of the Walker circulation over the Australian region, below average atmospheric pressure and above average convection over the summer hemisphere of the region, near-neutral values of the southern oscillation index, a weak and narrow zone of cool sea-surface temperatures in the equatorial eastern Pacific, weak warm sea-surface temperature anomalies in the northwestern Pacific and northern Australia, as well as an active monsoon over Asia. Four major active phases of the 30 to 60-day intraseasonal oscillation were observed, with periodicity apparently fluctuating between about 30 and 50 days. A total of 22 tropical cyclones developed during the period, less than the mean for the area. No cyclones formed in the south Pacific and south Indian Ocean (mean 2.8 ) for the season.**

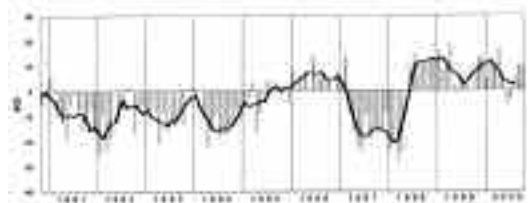
## Introduction

This summary reviews the broadscale tropical circulation in the Australian/Asian region during the period May to October 2000. The area covered is the Darwin Regional Specialised Meteorological Centre (RSMC) analysis domain, that is 70°E to 180°, 40°N to 40°S. Seasons such as those of 1999 and 1998 were described in previous summaries in this series, by Shaik and Bate (2000a) and Bate (1999) respectively. The first section uses mostly six-month average charts to describe the overall seasonal circulation and anomalies. The second section uses time series to portray variations of the tropical circulation within the season. Intraseasonal variability of various elements such as outgoing long wave radiation (OLR), 200 hPa velocity potential and mean sea-level pressure (MSLP) anomaly is analysed in this section. The third section briefly describes the occurrence of tropical cyclones in the six-month period.

## Data sources

The six-month seasonal charts were constructed using GASP, the Australian global model (see Appendix). Anomalies are derived from the European Centre for Medium-range Weather Forecasts (ECMWF) climatology. Sea-surface temperature (SST) anomalies were calculated relative to the 1°x1° global SST climatology from the US National Centers for Environmental Prediction (Reynolds and Smith 1995). Further details of the data sources used are listed in the Appendix.

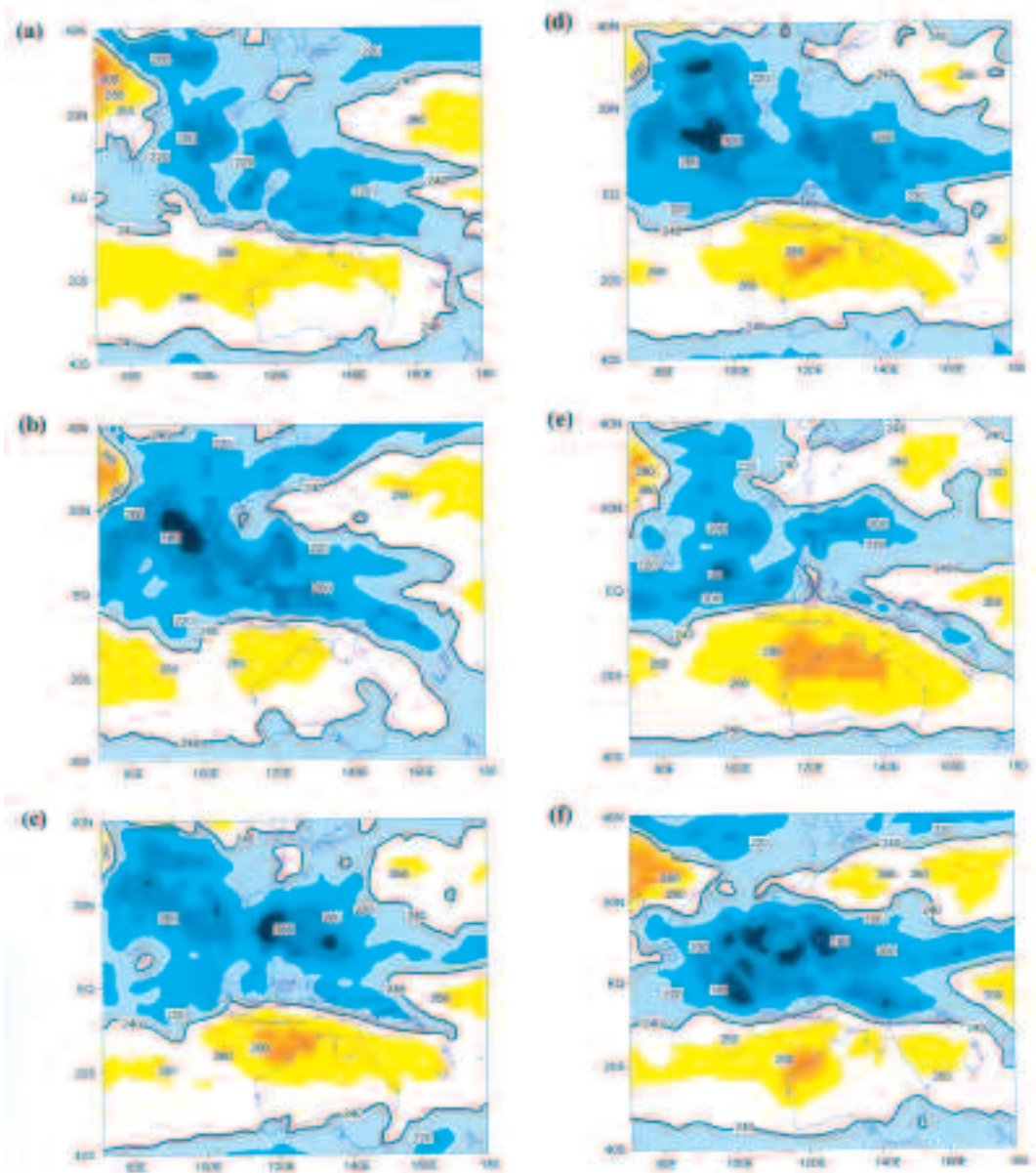
**Fig. 1** SOI time series for ten years to October 2000: monthly values (bars); five-month centred mean values (black line).



Corresponding author's address: Dr Hakeem A Shaik, PO Box 40050, Casuarina, NT 0811, Australia.  
email: H.shaik@bom.gov.au

**Table 1. Monthly values of Troup's SOI for the period January 1998 to October 2000.**

Year	Jan	Feb	Mar	Apr	May	Jun	Jul	Aug	Sep	Oct	Nov	Dec
1998	-24	-19	-29	-25	0	+10	+15	+10	+11	+11	+13	+13
1999	+16	+9	+9	+18	+2	+1	+5	+2	0	+9	+13	+13
2000	+5	+13	+9	+17	+4	-5	-4	+5	+10	+10		

**Fig. 2 Monthly mean OLR ( $W m^{-2}$ ), heavy line  $240 W m^{-2}$ ,  $260 W m^{-2}$  and above yellow-red shading,  $240 W m^{-2}$  and below, blue shading: (a) May 2000; (b) June 2000; (c) July 2000; (d) August 2000; (e) September 2000; (f) October 2000.**

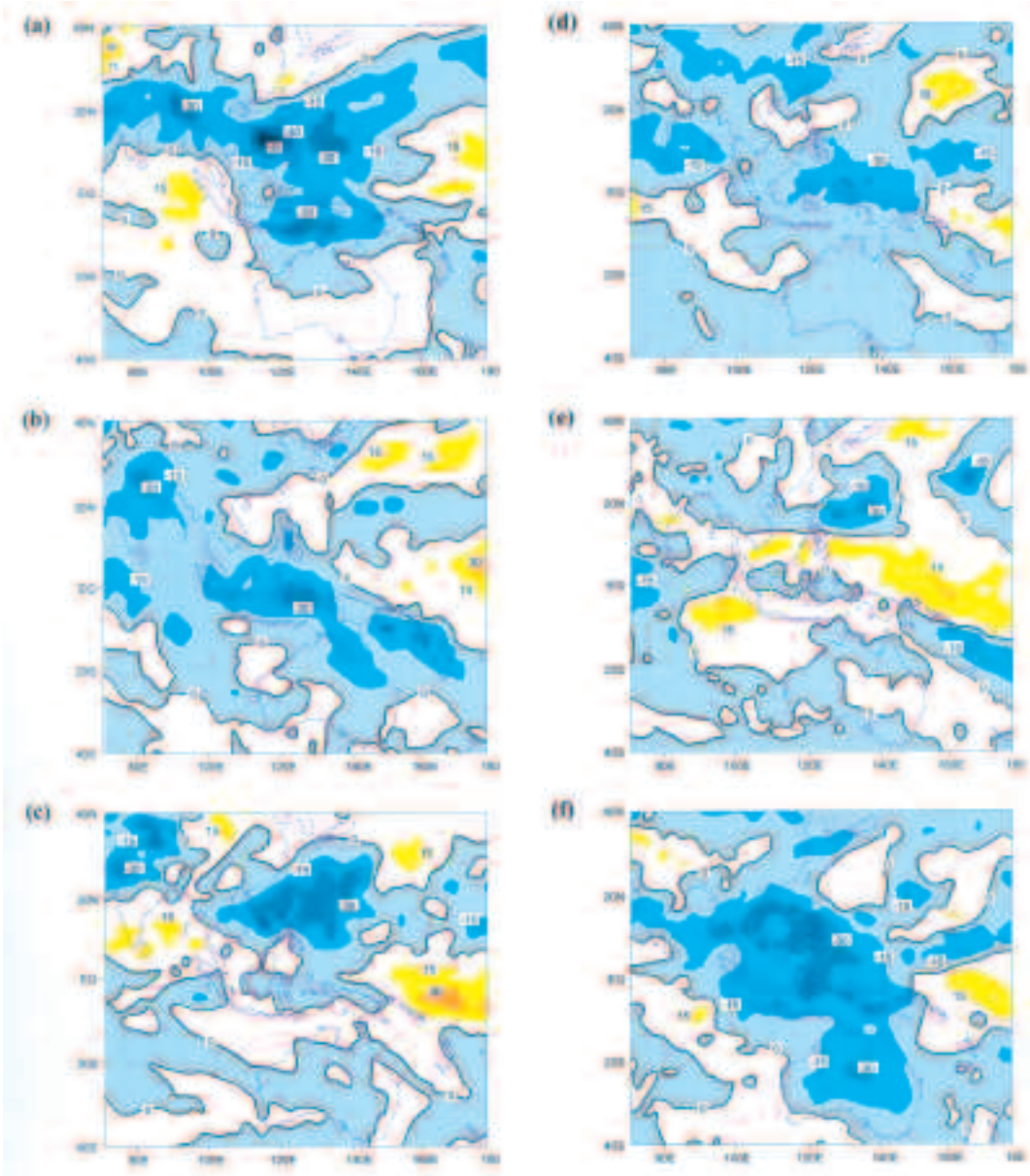
### Broadscale seasonal features

#### Southern Oscillation

Figure 1 shows the ten-year behaviour of Troup’s Southern Oscillation Index (SOI) from 1991 and its symmetrical five-month running mean. Monthly values of the SOI from January 1998 are given in Table 1. The La Niña conditions which continued from

1998 (Bate 1999) showed a weakening trend with a sizable fall in the SOI in May. It then oscillated between positive and negative low values during the first four months of the season. Though the SOI rose to +10 during September and October, the five-month running means of SOI remained close to the neutral range indicating the continuation of La Niña conditions along with other ENSO indicators.

**Fig. 3** Monthly OLR anomaly ( $W m^{-2}$ ), heavy line zero,  $> +15 W m^{-2}$  yellow-red shading,  $< zero W m^{-2}$ , blue shading; (a) May 2000; (b) June 2000; (c) July 2000; (d) August 2000; (e) September 2000; (f) October 2000. Anomalies from 1979-95 climatology.



### Convection and tropospheric circulation

The mean and anomaly of OLR – used as a proxy for convection – for each month are shown in Figs 2(a) to (f) and 3(a) to (f) respectively. Tropical convection anomalies were similar to the previous two six-month seasons (Shaik and Bate 2000a, 2000b). As expected in a La Niña event, tropical convection was generally above average (negative OLR anomalies) throughout the period over RSMC northern latitudes though less strongly evident in September. Weak positive OLR anomalies were evident over the western Pacific near the equator. OLR over India and most of southeast Asia indicate prolonged convection associated (in the northern hemisphere) with an early monsoon anchoring over central parts of India during June (Sinha Ray and Mukhopadhyay 2000). Though the areal extent of convection during much of the present season was comparable to that of 1998 and 1999 (Bate 1999; Shaik and Bate 2000a), the anomalies were weaker. Both the current season and 1999 season were preceded by positive SOI values and weak La Niña conditions whereas the 1998 season was preceded by moderate negative SOI values and El Niño conditions.

Velocity potential analyses at 850 hPa and 200 hPa (Fig. 4) are more or less similar to the previous year (Shaik and Bate 2000a) in terms of good vertical alignment of axes of maximum low-level convergence and upper-level divergence, indicating well organised up-motion and a vigorous Hadley cell, with active monsoon conditions in the northern hemisphere. They also show well aligned axes in the vicinity of the South Pacific convergence zone where convection was above average in most months. The axis at 850 hPa was better defined than in the long-term climatology and was associated with the monsoon trough in the northern hemisphere, extending almost parallel to the equator through southern parts of India, Thailand and Indonesia. The position of both low-level and upper-level axes remained close to the mean, coherent with continuing near normal or weak La Niña conditions (Shaik and Bate 2000a).

Mean sea-level pressure (MSLP) and anomalies are shown in Fig. 5. Pressures were generally below average, consistent with weak La Niña conditions. The overall pattern and position of subtropical highs were close to the mean. Over Australia the subtropical high was a little weaker than the mean while east of Japan it was slightly stronger than normal. Pressure anomalies were close to zero over much of the western equatorial Pacific and southern Indian Ocean, similar to the previous year (Shaik and Bate 2000a). Negative anomalies over India and east Asia reflect the active monsoon conditions in the area.

Vector wind analyses and anomalies at 850 hPa and 200 hPa are shown in Figs 6 and 7 respectively.

**Fig. 4** Six-month mean velocity potential ( $10^6 \text{ m}^2 \text{ s}^{-1}$ ), May to October 2000, negative contours dashed: (a) 850 hPa; (b) 200 hPa.

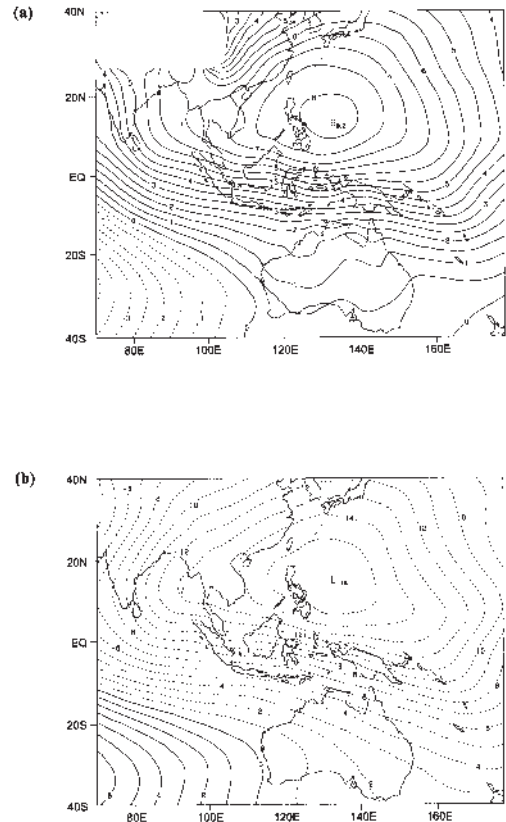


**Fig. 5** Six-month MSL pressure (hPa), May to October 2000: (a) mean, isobar interval 2 hPa; (b) anomaly, contour interval 1 hPa, shaded areas negative.

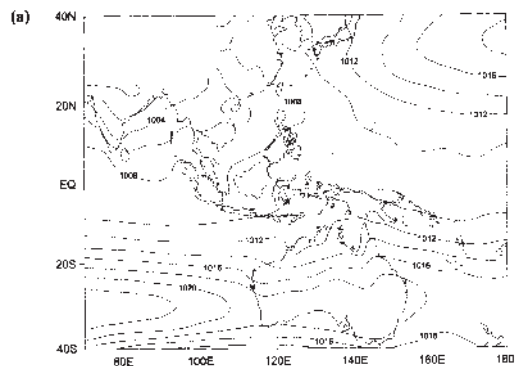


Fig. 5 Continued

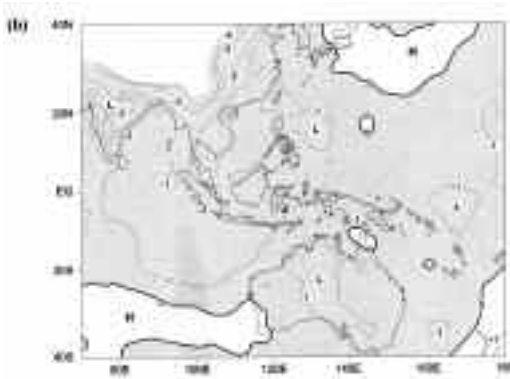
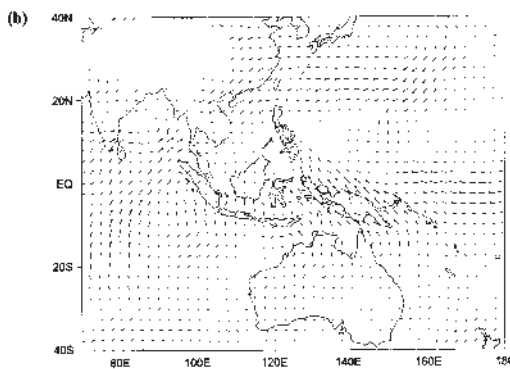
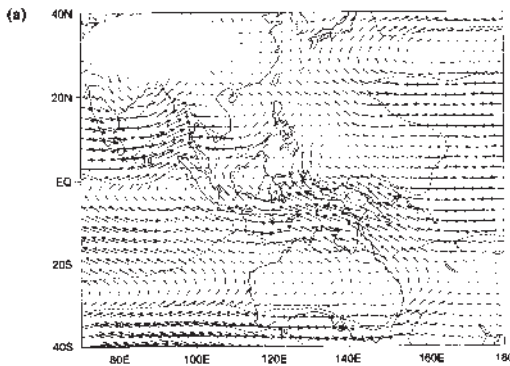
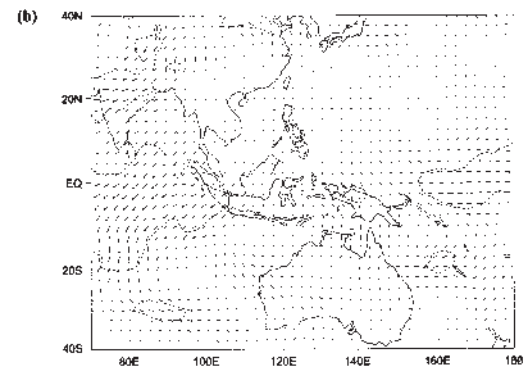
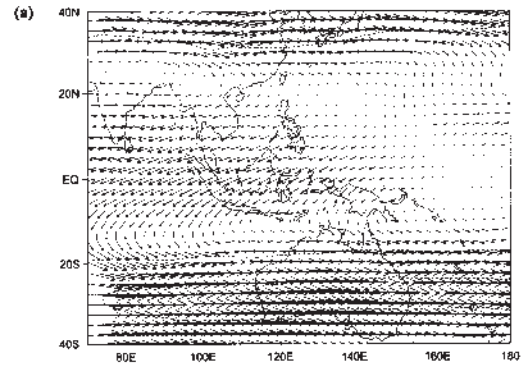


Fig. 6 Five-month 850 hPa vector wind field, June to October 2000, isotach (dashed) interval  $5 \text{ m s}^{-1}$ : (a) mean; (b) anomaly.



Though Figs 6 and 8 (cross-equatorial component) were available for the five-month period (June 2000 to October 2000) only, inference was drawn from the monthly *Darwin Tropical Diagnostic Statements*

Fig. 7 Six-month 200 hPa vector wind field, May to October 2000: (a) mean, isotach (dashed) interval  $20 \text{ m s}^{-1}$ ; (b) anomaly, isotach (dashed) interval  $5 \text{ m s}^{-1}$ .



(DTDS - see Appendix) for the whole season. The wind patterns were similar to those of the 1999 season (Shaik and Bate 2000a). The intertropical convergence zone was well-defined, with stronger than normal southwesterlies at 850 hPa level in the equatorial Indian Ocean. The monsoon trough was virtually non-existent east of the Philippines. The northwestern and equatorial western Pacific were dominated by easterly anomalies overlain by upper-level westerly anomalies, typical of La Niña. At the 200 hPa level, the subtropical westerlies in both hemispheres were close to the mean, while northeasterly anomalies in the north Indian Ocean indicate favourable upper outflow from the active monsoon in the region. The westerly anomalies in the equatorial Pacific west of the date-line were weaker, consistent with a weaker La Niña pattern.

Diagrams depicting the cross-equatorial component of the flow and anomalies (Fig. 8) indicate a pattern similar to the previous year with stronger than average cross-equatorial southerlies at the lower levels and stronger northerlies at upper levels, especially

**Fig. 8** Equatorial cross-section of five-month meridional wind, June to October 2000; contour interval  $2 \text{ m s}^{-1}$ , negative (northerly) contours dashed, positive (southerly) blue shading: (a) mean; (b) anomaly.

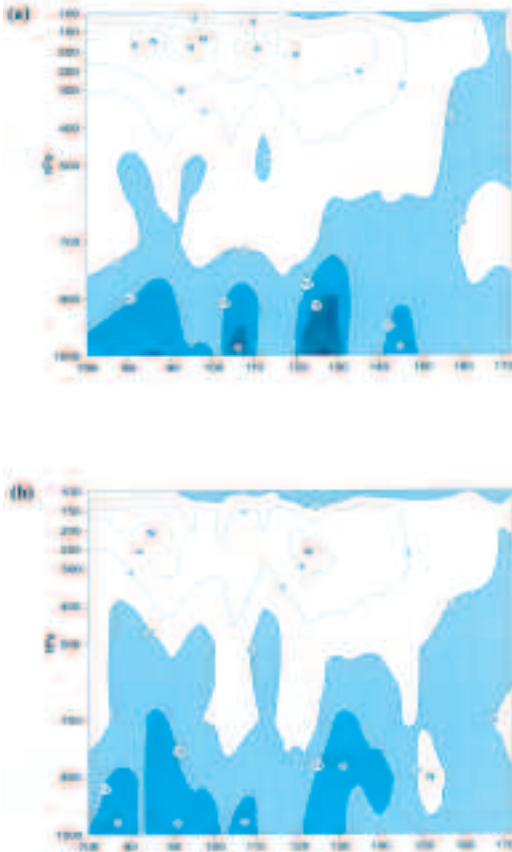
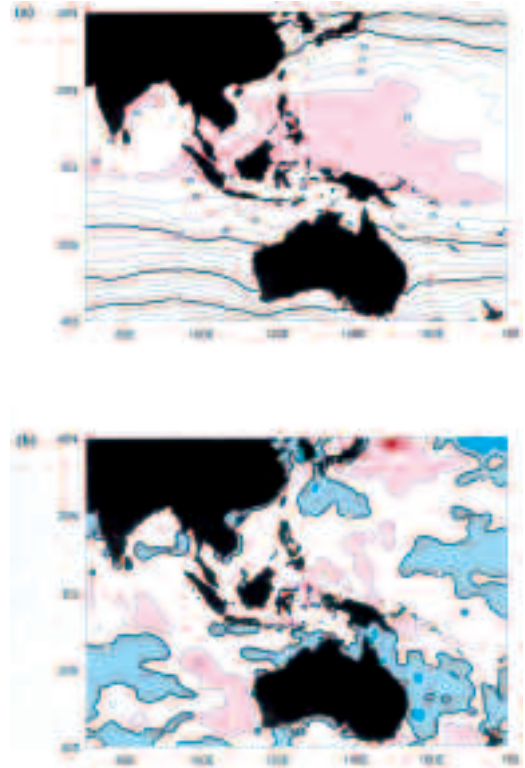


**Fig. 9** Six-month SST ( $^{\circ}\text{C}$ ), May to October 2000: (a) mean, isotherm interval  $1^{\circ}\text{C}$ ,  $>29^{\circ}\text{C}$  pink shading; (b) anomaly, contour interval  $0.5^{\circ}\text{C}$ ,  $< \text{zero } ^{\circ}\text{C}$  blue shading,  $> +0.5^{\circ}\text{C}$ , pink shading.



in the central and western parts of the RSMC domain. This supports the enhanced convection and Hadley cell associated with La Niña conditions.

### Sea-surface temperature

Six-month mean and anomalous sea-surface temperatures (SST) are shown in Fig. 9. Though the SST configuration shows a La Niña pattern, it is weaker than for the previous two seasons (Shaik and Bate 2000a, 2000b). Indicators of this change in Fig. 9 include: warm anomalies less extensive in the tropical north-western Pacific and cool anomalies about northern Australia; warm anomalies a year ago in the south-western Pacific were replaced by weak cool anomalies; weaker warm anomalies off the west coast of Western Australia. The confinement of cool anomalies in the equatorial eastern Pacific to a narrow zone east of  $160^{\circ}\text{W}$  (not shown) was also consistent with this change.

### Intraseasonal variability

Figures 10 to 12 show time/longitude plots of (a) 200 hPa velocity potential, (b) OLR and (c) MSLP anomaly, averaged over  $10^{\circ}$  latitude bands, across the Darwin RSMC longitude range. The northern OLR plot (Fig. 12(b)) also indicates the date and longitude of tropical cyclone genesis events.

Equatorial OLR series indicate several eastward propagating cloud structures mostly west of  $160^{\circ}\text{E}$ . Periodic behaviour is most clearly evident in the 200 hPa velocity potential and MSLP series. They diagnose the principal active periods beginning in early June, early July, early to mid-August and late September to early October. The 30 to 60-day (Madden-Julian) intraseasonal oscillation (ISO) signal is clear in these series. The periodicity in the early season was at the lower end of the ISO scale, around 30 days, but later pulses had a mean period of around

Fig. 10 Time-longitude sections, latitude band 5°S-15°S, 1 May 2000 to 31 October 2000 of five-day backward running mean: (a) 200 hPa velocity potential ( $10^5 \text{ m}^2 \text{ s}^{-1}$ ); (b) OLR ( $\text{W m}^{-2}$ ); (c) MSLP anomaly (hPa).

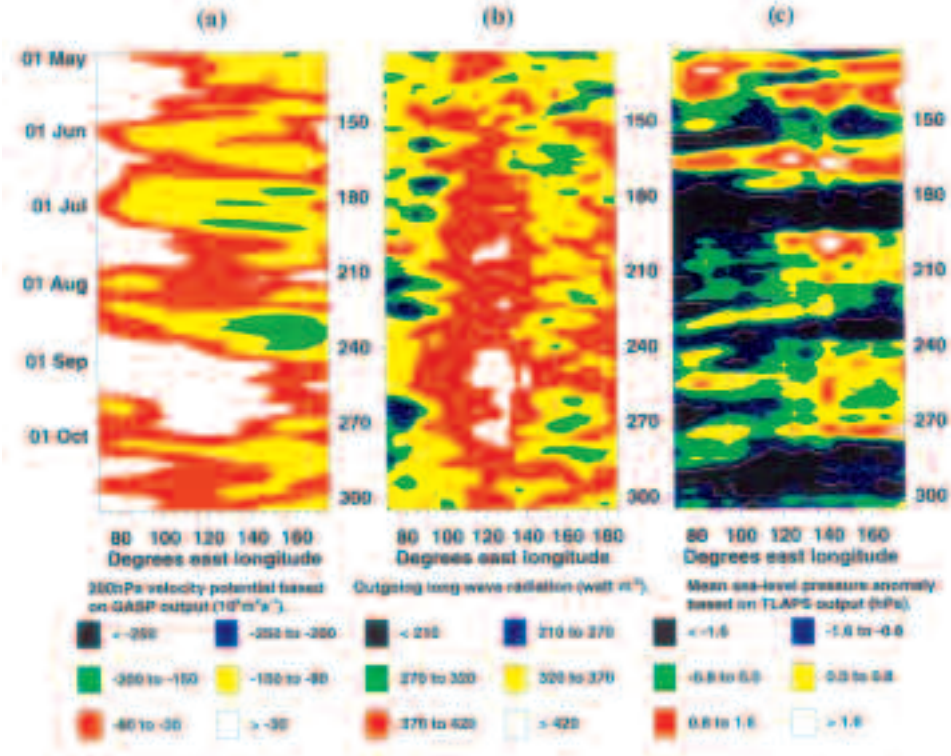


Fig. 11 As for Fig. 10, except latitude band 5°S-5°N.

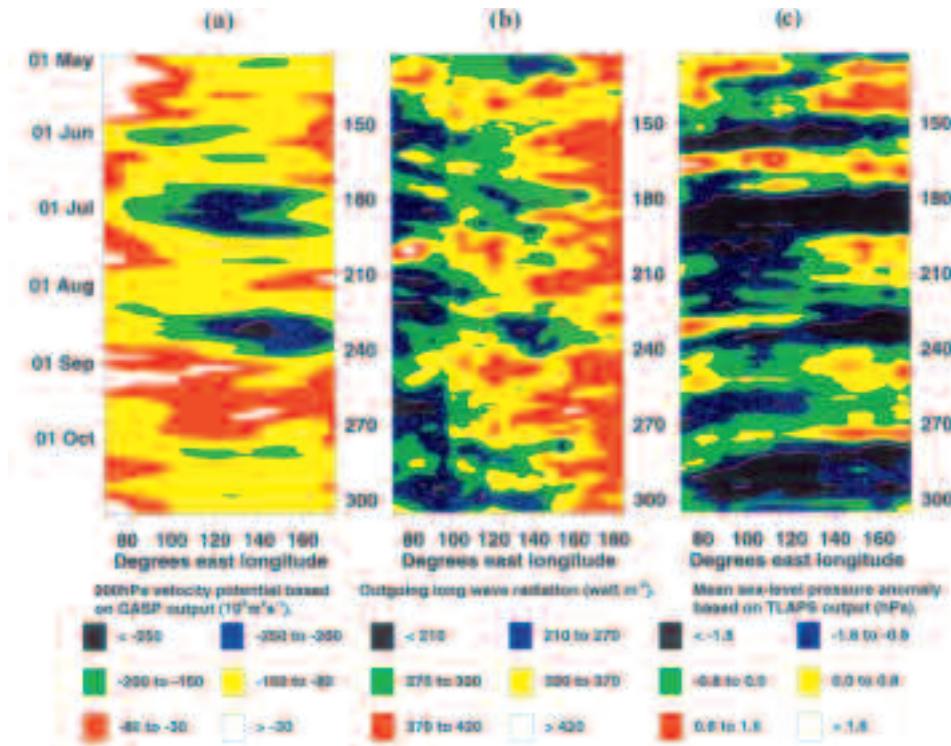
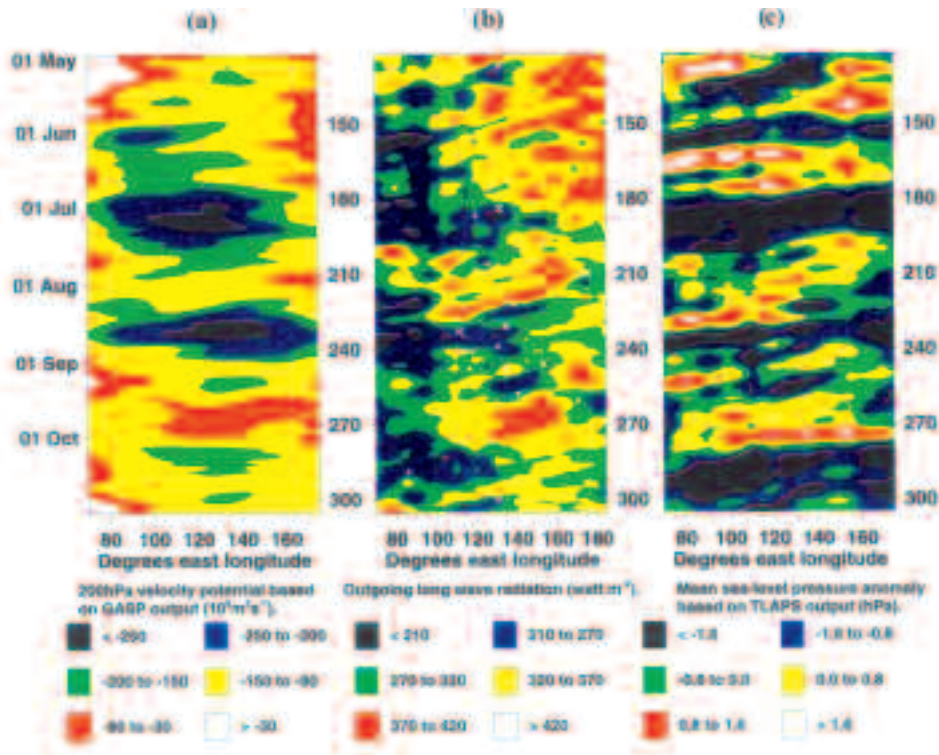


Fig. 12 As for Fig. 10, except latitude band 5°N-15°N. White crosses denote time and longitude of TC genesis events; dots denote events poleward of the latitude band.



50 days. The OLR series show generally cloudy conditions west of 140°E at equatorial latitudes and to a lesser extent, southern latitudes, while much of the northern region was cloud covered throughout the period. Also evident in northern and equatorial OLR and MSLP series are a number of shorter period westward-propagating features, corresponding generally to individual convective clusters or circulations. However, these were associated in some cases with higher frequencies of comparable amplitude such as equatorial Rossby waves.

Figure 13 shows filtered station pressure anomaly series for four stations, two in each hemisphere. In Fig. 13(c) the signal for the eastern station in each hemisphere has been added to that for the western station four days earlier. A four-day period was chosen as this is approximately the time that an eastward-moving global wave with a period of 45 days will take to travel over this longitude range. The pressures show major phase differences for all the four stations between August and September but were in good agreement over the rest of the period. Figure 13(c) generally supports the Hovmöller series

figures (Figs 10 to 12) coinciding more or less with the active phases of convection during early June, early July, early to mid-August and late September to early October. This is despite the strong evidence of higher frequency modes in the pressure anomaly time-longitude series.

## Tropical cyclones

Tropical cyclones (TC) are defined as having maximum ten-minute mean winds greater than  $17 \text{ m s}^{-1}$ , or named systems. Operational tracks are shown in Fig. 14, while Table 2 lists TCs in order of occurrence within the various basins, showing duration and estimated maximum intensity details. Tracks are from the near real-time publication DTDS, and are based on Darwin RSMC operational manual analyses, with limited post-analysis in a few cases.

Following WMO guidelines (Neumann 1993), winds are assumed to be averaged over ten minutes. Since most agencies use the unit of knots (kn) in warnings, wind speeds are shown in Table 2 in knots as well

**Fig. 13** MSLP anomalies for two tropical stations in each hemisphere, normalised then passed through a 40-day Butterworth filter, 50% response at 23 and 70 days: (a) southern hemisphere, thin line Cocos Island (12.2°S, 96.8°E), thick line Darwin (12.4°S, 130.9°E); (b) northern hemisphere, thin line Singapore (1.4°N, 104.0°E), thick line Yap (9.5°N, 138.1°E); (c) Darwin plus Cocos I four days earlier (thin line) and Yap plus Singapore four days earlier (thick line).

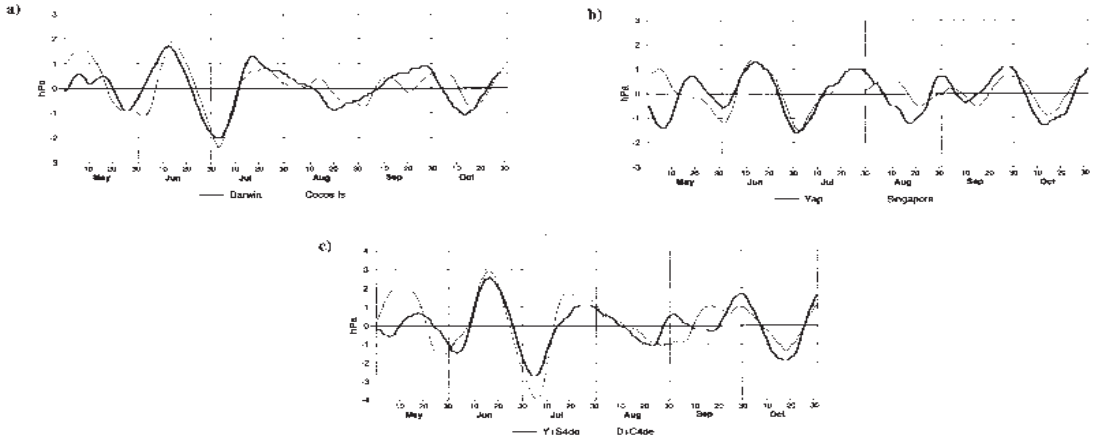


**Fig. 14** Tropical cyclone tracks, May to October 2000. Solid line denotes system reached severe tropical cyclone (typhoon) intensity; dashed line denotes system reached only tropical cyclone/storm intensity.

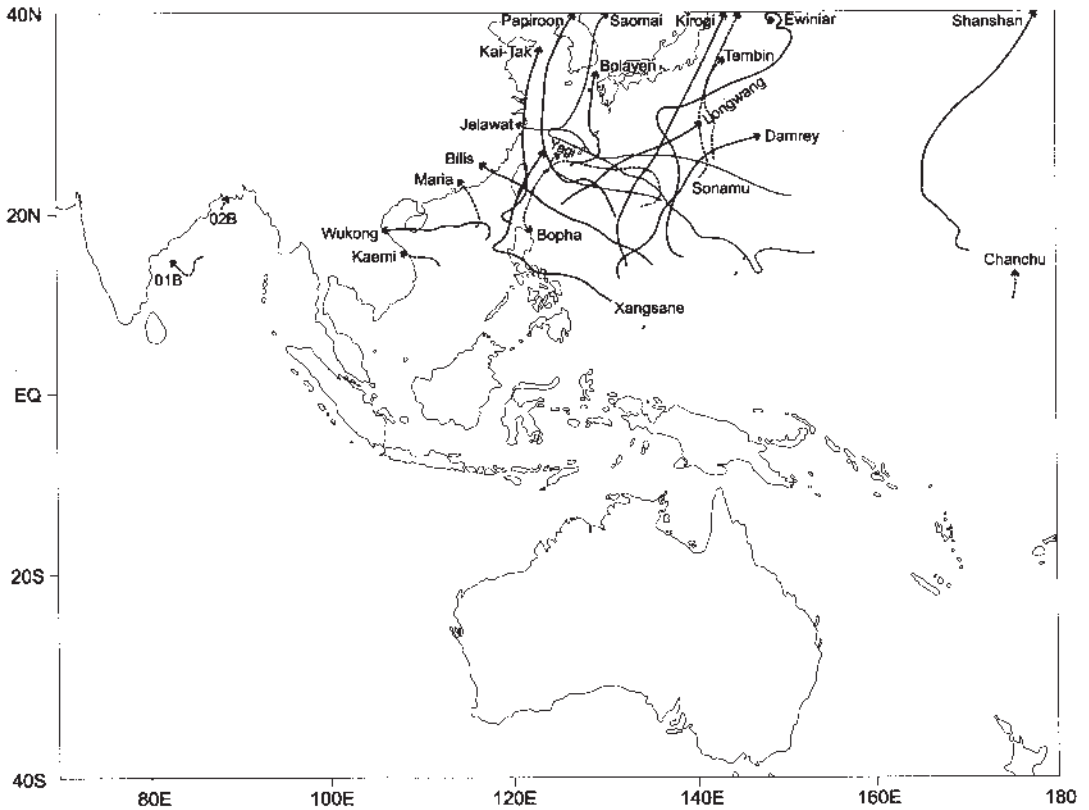


**Table 2. Tropical cyclones within the Darwin RSMC area, May to October 2000. TC = tropical cyclone, TS = tropical storm, Ty = typhoon.**

<i>Name</i>	<i>Dates (UTC) at TC intensity in Darwin RSMC area</i>	<i>Maximum* wind <math>m s^{-1}</math> (knots)</i>	<i>Estimated minimum MSLP (hPa)</i>	<i>Warning Agency**</i>
<i>Bay of Bengal/North Indian Ocean</i>				
01B (TC)	16 Oct - 18 Oct	18 (35)	997	IMD <sup>1</sup>
02B (TC)	27 Oct - 28 Oct	18 (35)	997	IMD <sup>1</sup>
<i>Northwest Pacific / South China Sea</i>				
Damrey (Ty)	6 May - 12 May	46 (90)	940	PAGASA Manila
Longwang (TS)	19 May - 20 May	23 (45)	992	JMA Tokyo
Kirogi (Ty) <sup>2</sup>	3 Jul - 8 Jul	46 (90)	940	PAGASA Manila
Kai-Tak (Ty)	5 Jul - 10 Jul	33 (65)	970	PAGASA Manila
Tembin (TS)	19 Jul - 22 Jul	21 (40)	992	JMA Tokyo
Bolaven (TS)	25 Jul - 30 Jul	28 (55)	980	JMA Tokyo
Chanchu (TS)	28 Jul - 29 Jul	18 (35)	994	JMA Tokyo
Jelawat (Ty)	1 Aug - 10 Aug	44 (85)	945	JMA Tokyo
Ewiniar (Ty) <sup>3</sup>	9 Aug - 19 Aug	36 (70)	965	JMA Tokyo
Bilis (Ty)	19 Aug - 23 Aug	57 (110)	915	JMA Tokyo
Kaemi (TS)	21 Aug - 22 Aug	23 (45)	985	Hong Kong
Prapiroon (Ty) <sup>4</sup>	26 Aug - 31 Aug	36 (70)	965	PAGASA Manila
Maria (TS)	29 Aug - 1 Sep	26 (50)	985	Hong Kong
Saomai (Ty) <sup>5</sup>	3 Sep - 16 Sep	49 (95)	925	JMA Tokyo
Wukong (Ty)	5 Sep - 10 Sep	33 (65)	970	PAGASA Manila
Bopha (TS)	5 Sep - 11 Sep	26 (50)	985	PAGASA Manila
Sonamu (TS) <sup>6</sup>	15 Sep - 17 Sep	28 (55)	980	JMA Tokyo
Shanshan (Ty) <sup>7</sup>	18 Sep - 24 Sep	49 (95)	935	JMA Tokyo
Yagi (Ty)	22 Oct - 26 Oct	33 (65)	975	JMA Tokyo
Xangsane (Ty)	26 Oct - 1 Nov	39 (75)	960	JMA Tokyo

\* Maximum 10-min. Mean wind while in Darwin RSMC area.

\*\* JMA = Japan Meteorological Agency; PAGASA = Philippine Atmospheric, Geophysical and Astronomical Services Administration.

Note that central pressures are not available from PAGASA Manila warnings; in these cases only the wind has been obtained from the warnings and pressures are estimated from the relationship of Atkinson and Holliday (1977)

#### Notes

1 India Meteorological Department track data from Sinha Ray and Mukhopadhyay (2001). Cyclone name and wind data are obtained from Joint Typhoon Warning Center, Pearl Harbor and pressures were estimated from the relationship of Atkinson and Holliday (1977)

2 Kirogi weakened, moved northeast out of RSMC area and caused a number of deaths in Japan.

3 Ewiniar weakened before moving out of RSMC area and later became extratropical.

4 Prapiroon moved north out of RSMC area and caused damage about Korea and east China.

5 Saomai moved out of RSMC area and became extratropical.

6 Sonamu moved north northeast and became extratropical.

7 Shanshan moved north-northeast out of RSMC area and became extratropical.

as  $m s^{-1}$ . Minimum pressures were obtained from the operational warnings, except for those issued by PAGASA Manila. In these cases minimum pressures were estimated using the relationship of Atkinson and Holliday (1977). Climatological numbers are from McPherson and Zettlemyer (2001) for the northwest Pacific and Mandal (1991) for the Bay of Bengal. A brief discussion and further details of each cyclone can be found in DTDS for the relevant month.

A total of 22 TC were analysed in the Darwin RSMC area during the summary period. The total number of cyclones was two less than the previous northern summer (Shaik and Bate 2000a) and six more than for the northern summer of 1998 (Bate 1999), a period of La Niña after a mature El Niño phase during 1997-1998 southern summer (Cleland 1998). The average number of cyclones in the region for the season is around 28. Twenty TC occurred in

the northwestern Pacific and two in the north Indian Ocean, compared to averages of 21.9 and 2.8 respectively. Out of the twenty cyclones which formed in the northwestern Pacific twelve reached typhoon intensity (average 14.4 typhoons). No cyclones formed in the South Pacific and south Indian Ocean against a mean of 2.8 cyclones for the season.

## Acknowledgments

The authors would like to express their sincere thanks to Dr Rob Dahni, Bureau of Meteorology, Melbourne, for his generous help in improving some of the time series figures using his IDL programming skills. Sincere thanks are also due to Rob Porteous for his drafting of various figures and Gordon Jackson for generating the six-month averages. Thanks are also expressed to the Climate Prediction Center, Camp Springs, Maryland, USA, for permission to use OLR figures.

## Appendix

Data sources used in this summary were:

*Darwin Tropical Diagnostic Statement*, May to October 2000 (issued monthly), and *Weekly Tropical Climate Note*, 2 May 2000 to 31 October 2000. Bureau of Meteorology, PO Box 40050, Casuarina, NT 0811, Australia.

MSLP, upper wind and velocity potential map fields from the Australian Bureau of Meteorology's Global Assimilation and Prediction system (GASP - Bourke et al. 1990; Bureau of Meteorology 1998); anomalies derived from the ECMWF 30-year climatology. MSLP and velocity potential data for Hovmöller series from the Limited Area Prediction System (LAPS - Puri et al. 1998), nested within GASP.

OLR monthly map figures from *Climate Diagnostics Bulletin*, May to October 2000, issued monthly by Climate Prediction Center, W/NP52, Room 605, WWBG, 5200 Auth Road, Camp Springs, Maryland, 20746-4304 USA. OLR data for Hovmöller diagrams from Japan Meteorological Agency's GMS-5 geostationary satellite.

Sea-surface temperature analysis derived from the operational global analysis of National Meteorological and Oceanographic Centre, Bureau of Meteorology, Melbourne. Includes blended *in situ* and satellite data, 1°C resolution. The 1°x1° global

SST climatology from the US National Centers for Environment Prediction (Reynolds and Smith 1995) was used to calculate anomalies.

Tropical cyclone climatology for the northwest Pacific Ocean calculated from figures given in McPherson and Zettlemyer (2001). For the north Indian Ocean the climatology is from Mandal (1991).

## References

- Atkinson, G.D. and Holliday, C.R. 1977. Tropical cyclone minimum sea level pressure/maximum sustained wind relationship for the western north Pacific. *Mon. Weath. Rev.*, 105, 421-7.
- Bate, P.W. 1999. The tropical circulation in the Australian/Asian region - May to October 1998. *Aust. Met. Mag.* 48, 45-54.
- Bourke, W., Seaman, R., Embery, G., McAvaney, B., Naughton, M., Hart, T. and Rikus, L. 1990. The BMRC global assimilation and prediction system. *ECMWF Seminar Series: Ten years of medium-range weather forecasting*. 4-8 September 1989, 221-52.
- Bureau of Meteorology 1998. Upgrade of the Global Analysis and Prediction (GASP) system. *Analysis and Prediction Operations Bulletin No 45*. Bur. Met., Australia, 16pp.
- Cleland, S.J. 1998. The tropical circulation in the Australian/Asian region - November 1997 to April 1998. *Aust. Met. Mag.*, 47, 243-52.
- Mandal, G.S. 1991. Tropical cyclones and their forecasting and warning systems in the Indian Ocean. *Technical Document WMO/TD - No. 430 (Report No. TCP-28)*, WMO, Geneva, 430pp.
- McPherson, T. and Zettlemyer, M. 2001. *2000 Annual Tropical Cyclone Report*, US Naval Pacific Meteorology and Oceanography Center/ Joint Typhoon Warning Center, Pearl Harbor, Hawaii, USA, 399 pp. (A PDF version on web at [http://www.npmoc.navy.mil/products/jtwc/2000\\_atcr/](http://www.npmoc.navy.mil/products/jtwc/2000_atcr/)).
- Neumann, C.J. 1993. The global tropical cyclone forecasting network. In: *Global Guide to Tropical Cyclone Forecasting. Technical Document WMO/TD - No. 560 (Report No. TCP-31)*, WMO, Geneva.
- Puri, K., Dietachmayer, G., Mills, G.A., Davidson, N.E., Bowen, R.A. and Logan, L.W. 1998. The new BMRC Limited Area Prediction System, LAPS. *Aust. Met. Mag.*, 47, 203-23.
- Reynolds, R.W. and Smith, T.M. 1995. A high resolution global sea surface temperature climatology. *J. climate*, 8, 1571-83.
- Shaik, A.H. and Bate, P.W. 2000a. The tropical circulation in the Australian/Asian region - May to October 1999. *Aust. Met. Mag.* 49, 59-69.
- Shaik, A.H. and Bate, P.W. 2000b. The tropical circulation in the Australian/Asian region - November 1999 to April 2000. *Aust. Met. Mag.* 49, 331-42.
- Sinha Ray, K.C. and Mukhopadhyay, R.K. 2000. Climate Diagnostic Bulletin of India - Seasonal, Monsoon season (June-September) - 2000, National Climate Centre, India Meteorological Department, Pune, India. *Special issue No. 18*, 25pp.
- Sinha Ray, K.C. and Mukhopadhyay, R.K. 2001. Climate Diagnostic Bulletin of India - Seasonal, Post-Monsoon season (October-December) - 2000, National Climate Centre, India Meteorological Department, Pune, India. *Special issue No. 19*, 20pp.



# Numerical prediction model performance summary October to December 2000

W. Skinner and T. Hart

National Meteorological and Oceanographic Centre, Bureau of Meteorology,  
Australia

(Manuscript received April 2001)

## Introduction

This summary continues the series comparing the performances of numerical weather prediction (NWP) models.

## Models and methods

A description of the Australian verification methods can be found in a previous article (Skinner 1995).

Models are from the National Meteorological and Oceanographic Centre (NMOC) Melbourne and from ECMWF (European Centre for Medium-range Weather Forecasts), NCEP (National Centers for Environmental Prediction), UKMO (United Kingdom Meteorological Office) and JMA (Japan Meteorological Agency).

Four models considered from NMOC, Melbourne, are: LAPS\_PT375 (Limited Area Prediction System Point 375); MESO\_LAPS\_PT125 (MESOscale Limited Area Prediction System Point 125) TLAPS\_PT375 (Tropical Limited Area Prediction System Point 375); and GASP (Global Assimulation and Prediction).

Overseas global models included in the comparisons are: ECSP (ECMWF Spectral Assimilation); USAVM (NCEP Spectral Model for Aviation); UKGC (UK Meteorological Office grid PE model); and JMAGSM (JMA Global Spectral Model).

Very short summaries of the models can be found in the initial article (Skinner 1995) with references to model updates in subsequent issues.

All results have been calculated within NMOC Melbourne, where the models were verified against their own analyses. Results are presented for the irregular Australian verification area only (see Fig. 5).

The statistics are a measure of the skill in forecasting geopotential height at 500 hPa or mean sea-level pressure (MSLP). Other field types are not included in these summaries.

The limited area models are run several hours earlier than GASP and this premature data cut-off, particularly for satellite information, adversely affects their skill compared to GASP.

Note that the Australian region verification grid has southerly points which are outside the TLAPS\_PT375 grid and easterly points outside the MESO\_LAPS\_PT125 grid. TLAPS\_PT375 and MESO\_LAPS\_PT125 scores are calculated without these points and are therefore not strictly comparable with those from other models.

## Notes on NWP systems

### ECMWF

The resolution of the ECMWF global atmospheric prediction model was increased from  $T_L319$  to  $T_L511$  on 21 November 2000, described as roughly equivalent to a reduction from 60 km to 40 km grid size. The resolution of the data assimilation minimisation used in their 4DVAR analysis was increased from  $T63$  to  $T_L159$  on the same date. (The subscript is used to denote that the grid used for the calculations of non-linear dynamic terms and physics processes is at a lower resolution with the semi-Lagrangian time stepping algorithm than formerly used with the Eulerian scheme.)

The time schedule and types of products disseminated via GTS remain unchanged.

---

Corresponding author address: Ms Wilma Skinner, National Meteorological and Oceanographic Centre, Bureau of Meteorology, GPO Box 1289K, Vic. 3001, Australia.